Modeling of Flame Acceleration and DDT in Open-Ended Channel with Homogeneous Premixed H2-Air Mixture

Petar Bosnic, Mathias Henriksen, Dag Bjerketvedt, Knut Vaagsaether
Faculty of Technology, Natural Sciences and Maritime Sciences, University of South-Eastern Norway
Kjølnes Ring 56, Porsgrunn, 3901, Norway

1 Introduction

Accurately predicting pressure loads from hydrogen–air explosions, including deflagrations and detonations, is critical for evaluating hazards in hydrogen technologies. Hydrogen's low ignition energy, high reactivity, and wide detonability range significantly increase the likelihood of deflagration-to-detonation transition (DDT) compared to hydrocarbon–air mixtures. Obstacles enhance flame propagation by inducing vortex stretching and flame surface expansion, accelerating combustion and reducing the distance and time required for DDT [1]. Experimental studies provide important insights into DDT mechanisms but are often limited in scope. Computational fluid dynamics (CFD) is a valuable tool for studying flame acceleration (FA) and DDT, providing details about turbulent flame evolution and interactions with obstacles and shocks. However, CFD simulations must still be validated against experimental data to ensure reliability.

The objective of this study is to simulate the deflagration-to-detonation transition (DDT) using relatively coarse computational meshes to enhance its applicability in engineering applications. This work introduces a CFD framework in OpenFOAM 9 for simulating homogeneous hydrogen–air explosions using a reaction progress variable approach. Building on the methodology introduced by [2], the model incorporates source terms for deflagration, auto-ignition, and detonation. The initial implementation of this methodology in OpenFOAM was carried out by [3, 4]. Validation of the preliminary model is performed using experimental data from the University of South-Eastern Norway's Process Safety, Combustion, and Explosions Research Laboratory [5].

2 Numerical Model

2.1 Governing Equation

The general governing equations for the unsteady, compressible Navier-Stokes system are given by:

$$\frac{\partial \mathbf{U}}{\partial t} + \nabla \cdot \mathbf{F} = \mathbf{S}, \tag{1}$$

where:

$$\mathbf{U} = \begin{pmatrix} \rho \\ \rho \mathbf{u} \\ \rho E \end{pmatrix}, \quad \mathbf{F} = \begin{pmatrix} \rho \mathbf{u} \\ \rho \mathbf{u} \otimes \mathbf{u} + p\mathbf{I} \\ (\rho E + p)\mathbf{u} \end{pmatrix}, \quad \mathbf{S} = \begin{pmatrix} 0 \\ \rho \mathbf{g} + \nabla \cdot \tau \\ \dot{E} \end{pmatrix}. \tag{2}$$

Correspondence to: petar.bosnic@usn.no

Here, $\mathbf{U}$ is the vector of conservative variables, $\mathbf{F}$ is the flux vector and $\mathbf{S}$ is the source term vector. ρ represents the density, $\mathbf{u}$ is the velocity vector, E is the total energy per unit mass defined as $E = e + \frac{1}{2}|\mathbf{u}|^2$ with e as internal energy, p is the pressure, $\rho\mathbf{g}$ denotes the gravitational force, $\nabla \cdot \tau$ is the divergence of the stress tensor representing viscous forces, and $\dot{E}$ accounts for source terms of energy, such as heat addition or viscous dissipation.

2.2 Solver Basis

The solver employs a two-step approach originally developed in `blastFoam` [6] to solve the governing equations. First, primary variables (density, momentum, total energy, and internal energy) are updated explicitly using flux divergences computed with the HLLC approximate Riemann solver [7] and multi-dimensional slope limiters, ensuring stability based on the Courant–Friedrichs–Lewy (CFL) condition. Then, turbulence-induced stresses and thermal energy diffusion are incorporated via an implicit finite volume method to obtain the final solution.

2.3 Combustion Model

The progress variable c is used to describe the reaction zone in a premixed turbulent flame, where the product can exist in one of three states: unreacted ($c = 0$), fully reacted ($c = 1$), or a transitional state representing varying degrees of reaction. The progress variable c is commonly defined using properties like temperature or the mass fraction of reactants. This variable is constrained between specific values for the burned gas (T_b) and the fresh gas (T_f), as expressed by:

$$c = \frac{T - T_f}{T_b - T_f} \tag{3}$$

Weller's combustion model [8], instead introduces a transport equation for the reaction regress variable, b, where:

$$b = 1 - c \tag{4}$$

The solver uses transport equation for b given by:

$$\frac{\partial(\rho b)}{\partial t} + \nabla \cdot (\rho \mathbf{u} b) - \nabla \cdot \left(\frac{\mu_t}{Sc_t} \nabla b \right) = \begin{cases} \rho_u S_u \Xi |\nabla b|, & \tau < 0.99, \\ \rho \frac{1-b}{\Delta t}, & \tau \geq 0.99. \end{cases} \tag{5}$$

where the turbulent Schmidt number $Sc_T = 1.0$, the eddy viscosity μ_T is provided by the turbulence model, and S_u represents the laminar burning velocity determined using Guilder's formulation.

The algebraic model for Ξ is given by:

$$\Xi = 1 + \left(1 + 2 \cdot \Xi_{\text{ShapeCoef}} \cdot (0.5 - b)\right) \cdot \Xi_{\text{Coef}} \cdot \sqrt{\frac{u_p}{S_u + S_{u,\text{min}}}} \cdot R_\eta \tag{6}$$

The two-step approach for modeling auto-ignition, as proposed by [2, 3], is implemented. The first step models the isothermal induction time, while the second step accounts for the exothermic heat release. In equation (5), the source term for the reaction regress variable is dynamically chosen by the auto-ignition term τ, which is bounded between 0 and 1. While $\tau \leq 0.99$, certain cells have not yet reached auto-ignition and use the deflagration source term. Once the auto-ignition time expires or when $\tau > 0.99$, the exothermic source term takes over.

The auto-ignition induction time model predicts auto-ignition phenomena using a precomputed table based on pressure and unburned gas temperature, reducing computational costs while maintaining accuracy. The induction time and the auto-ignition term τ are defined as:

$$t_{\text{ind}} = t_{\text{ind}}(p, T_u, \phi), \quad \tau = \frac{t}{t_{\text{ind}}}. \tag{7}$$

The transport equation for τ is:

$$\frac{\partial(\rho\tau)}{\partial t} + \nabla \cdot (\rho \mathbf{u}\tau) - \nabla \cdot \left(\frac{\mu_t}{Sc_t} \nabla\tau \right) = \frac{\rho}{t_{\text{ind}}}. \tag{8}$$

Induction times (t_{ind}) are determined from multi-dimensional lookup tables generated using 0D isochoric explosion calculations with SDToolBox [9], and the detailed reaction mechanism by O'Conaire [10]. During simulations, t_{ind} is retrieved for each computational cell using current pressure and temperature values, bounded within predefined limits for numerical stability. This approach ensures efficient and robust modeling of auto-ignition phenomena without recalculating detailed chemical reactions.

2.4 Adaptive Mesh Refinement (AMR)

The solver integrates an Adaptive Mesh Refinement (AMR) library to dynamically refine or coarsen the computational grid based on the solution's requirements. This technique ensures high resolution in regions of interest, such as flame fronts, shock waves, and reaction zones, while maintaining computational efficiency in less critical areas. The AMR framework implemented in the solver is based on the load-balanced AMR library `blastAMR` [11].

2.5 Computational Setup

The experimental setup follows the geometry described in [5]: a $1000\,\text{mm}\,(L) \times 116.5\,\text{mm}\,(H) \times 65\,\text{mm}\,(D)$ open-ended channel with 40 cylindrical ($\Phi = 18\,\text{mm}$) obstacles, creating a blockage ratio of 77%, positioned 400 mm downstream of the ignition source. The gas mixture is a homogeneous hydrogen-air blend with 31.61 vol% hydrogen (equivalence ratio $\phi = 1.1$) at atmospheric conditions. Transport properties are computed using Sutherland's law, thermodynamic properties from JANAF tables, and the equation of state modeled as a perfect gas. Reactant and product properties, including molecular weight, transport coefficients (e.g., A_s and T_s), specific heat coefficients (NASA polynomials), and Gulder's correlation coefficients for laminar flame speed, were derived using `mech2Foam` [12]. Turbulence is modeled with the RANS k-ω SST model [13], with adaptive time stepping controlled by a CFL number of 0.4. Simulations were conducted on a uniform 2D grid using 6 CPU cores in parallel. Boundary conditions are defined as: - b, k, p, S_u, T, T_u, τ, and Ξ: `zeroGradient` at walls and outlet. - ω: `omegaWallFunction` at walls, `zeroGradient` at outlet. - $\omega_{\text{C,ign}}$: `calculated` at walls and outlet. - U: `noSlip` at walls, `pressureInletOutletVelocity` at outlet.

3 Results and Discussion

Numerical results from Case 2 are presented in Figure 1. As the flame exits the obstacle field, expansion and acceleration behind obstacles generate a leading shock wave due to rapid volumetric expansion of burned gases. Continued flame acceleration intensifies the pressure gradient, producing progressively stronger shock waves that precede the flame. At 8.192 ms, colliding shock waves compress the unreacted gas, locally raising pressure and temperature, thereby reducing the induction time and triggering

auto-ignition. While the current simulation lacks the resolution to fully capture fine-scale shock-flame interactions and boundary layer effects observed in high-resolution studies [1], it effectively represents the key mechanism: shock waves from multiple flame jets collide, inducing precompression and turbulence, which enhance mixing and the local reaction rate, leading to auto-ignition. A central hot spot forms and rapidly expands, consuming the precompressed mixture. At approximately 8.243 ms, the hot spot reaches the channel walls, where confinement and reflected shocks promote further compression and help initiate the DDT. The resulting interaction forms a Mach stem and reflected shock, increasing local pressure and flow confinement, further accelerating the reaction front and establishing a stable detonation regime characterized by a leading shock compressing the unburned mixture ahead of a narrow reaction zone.

Table 1: Summary of Simulation Cases

Case	Mesh	AMR	Base/Min. Mesh (mm)	Run Time (h)	DDT	$p_{3,\max}$ (bar)	$p_{4,\max}$ (bar)
1	26 152	Yes	2 / 0.5	21	Yes	29.5	24.7
2	116400	No	1 / 1	40	Yes	17.3	18.1
3	26 152	Yes	2 / 1	5	Yes	9.0	38.1
4	26 152	No	2 / 2	0.75	No	6.4	6.6

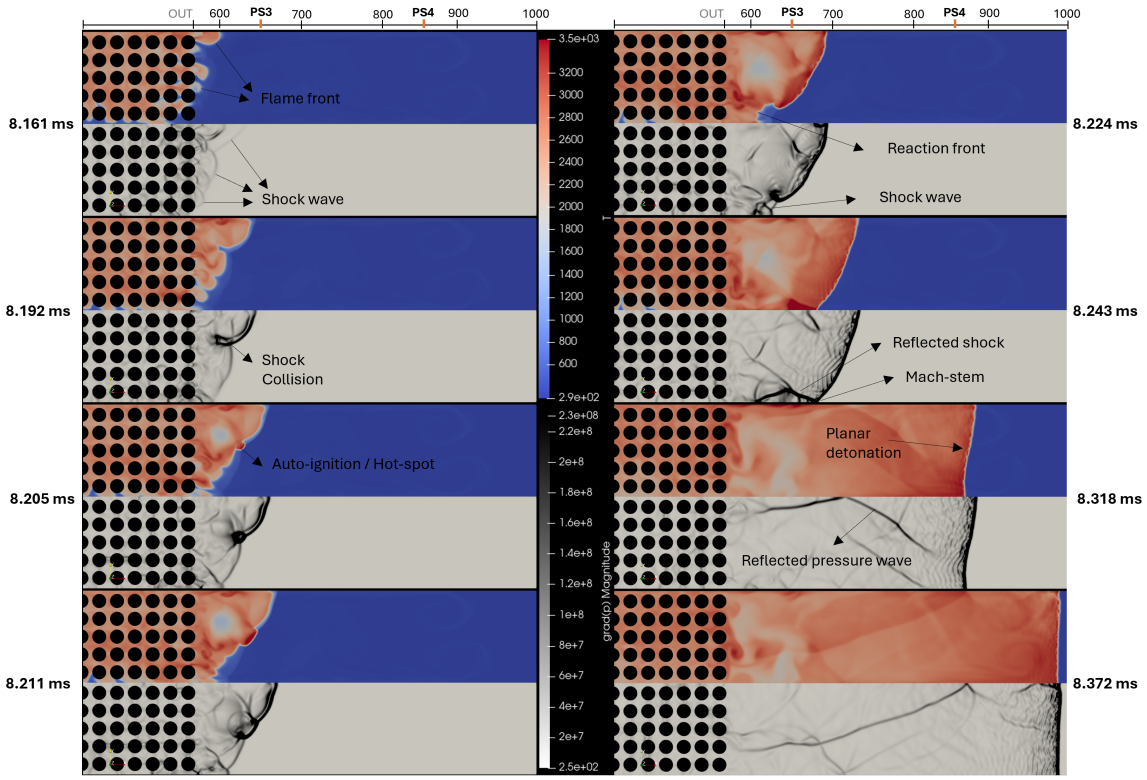

Figure 1: Onset of detonation: Numerical results for Case 2.

Figure 2 presents the overpressure measured by pressure sensors 3 and 4, along with the flame front velocities downstream of the obstacles. Upon exiting the obstacle field at approximately 600 m/s, the flame initially decelerates due to expansion into the open section. However, the flame soon accelerates again due to intensified combustion occurring behind and within the obstacle field, triggering a local auto-ignition. A rapid velocity increase to 2300–2500 m/s marks the onset of overdriven detonation, followed by relaxation to a Chapman–Jouguet (CJ) detonation. This sequence reflects a DDT process,

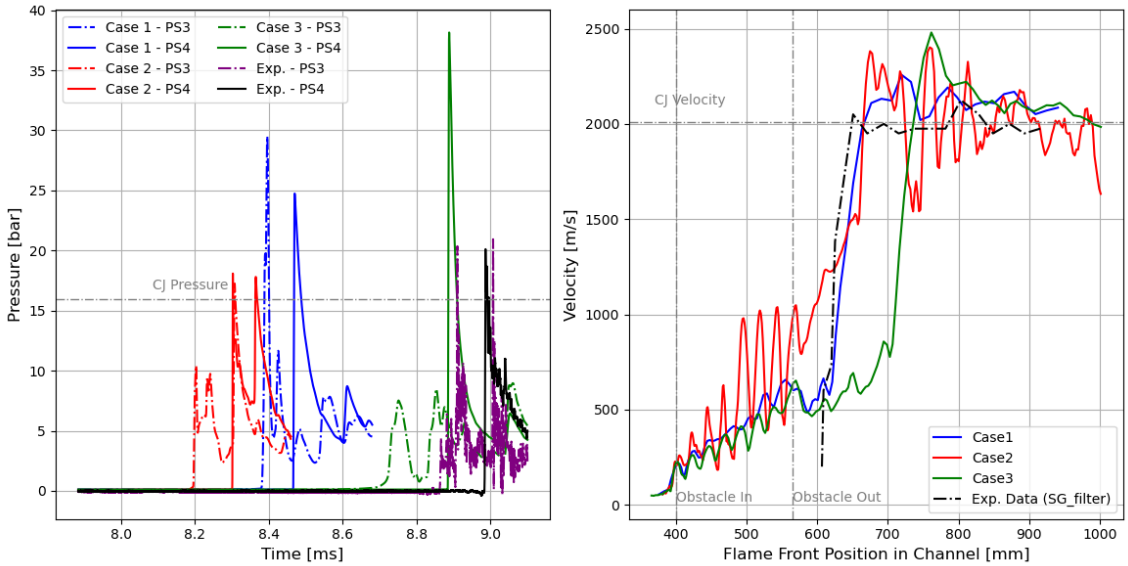

Figure 2: Overpressure measurements at the top wall and flame front velocity plot.

where the overdriven detonation transitions toward CJ conditions as the shock and reaction zone fully couple. The detonation wave is identified by a sharp pressure jump, with simulated peaks reaching 17–38 bar. In the presented experiment, pressure peaks of approximately 20–21 bars are observed, indicating a overestimation in the simulation. However, experimental pressure peaks vary significantly, depending on local shock structure (e.g., proximity to Mach stems or triple points). The reflected pressure wave, observed as a secondary peak, indicates strong wall interactions and pressure reinforcement behind the detonation. Figure 2 illustrates the solver's sensitivity to mesh resolution, especially in predicting the timing and location of detonation onset. Case 2 exhibits the most pronounced oscillations in flame front velocity, likely due to numerical instabilities caused by abrupt grid transitions or underresolved gradients. Both Case 1 and Case 2 successfully predict the DDT location, whereas Case 3 underpredicts it, likely due to insufficient resolution of the flame–shock interaction zone. Among all cases, Case 1 provides the best overall agreement with experimental data, as it is the only case that captures the detonation-induced pressure peak at sensor PS3, consistent with experimental observations. In all simulations, however, detonation velocities remain overestimated, exceeding the theoretical CJ values, possibly due to overdriven wave stabilization or an overactive detonation source term.

4 Conclusion

This paper presented a preliminary solver implemented in OpenFOAM 9 for simulating deflagration-to-detonation transition (DDT) in homogeneous premixed hydrogen–air mixtures. The combustion model included three source terms: deflagration, auto-ignition, and detonation, based on a progress variable formulation. The solver's results were validated against experimental data for a hydrogen-air mixture ($\phi = 1.1$). The numerical solver demonstrated good agreement with experimental data in predicting key aspects of the DDT process, including the mechanism of DDT via shock focusing, DDT location, overpressure characteristics, and flame front velocities. However, sensitivity to mesh size was evident. Case 4, which used a uniform 2 mm mesh without adaptive mesh refinement (AMR), failed to predict DDT. This may be due to numerical diffusion at coarse resolution, which smooths shock fronts and prevents the accurate buildup of post-shock conditions needed for auto-ignition. Conversely, Case 3 showed that refining the flame-shock complex with a 1 mm mesh enabled accurate DDT prediction. These findings

are promising for larger-scale simulations, where refining the shock-flame complex with a 1 mm mesh while coarsening other regions can significantly reduce computational costs without sacrificing accuracy. Although the solver captured DDT and stable detonation propagation, detonation velocities were consistently overestimated compared to CJ values. This suggests that the energy release may be overestimated, pointing to the need for refinement of the detonation source term and thermodynamic modeling. Since DDT and turbulence are inherently 3D phenomena, future solver development will prioritize 3D capabilities.

Acknowledgements: This publication has been produced with support from the HYDROGENi Research Centre (hydrogeni.no), performed under the Norwegian research program FMETEKN. The authors acknowledge the industry partners in HYDROGENi for their contributions and the Research Council of Norway (333118).

References

[1] Elaine S. Oran and Vadim N. Gamezo. "Origins of the Deflagration-to-Detonation Transition in Gas-Phase Combustion". In: *Combustion and Flame* 148.1–2 (Jan. 2007), pp. 4–47.

[2] K Vaagsaether, V Knudsen, and D Bjerketvedt. "Simulation of Flame Acceleration and DDT in H2H2-air Mixture with a Flux Limiter Centered Method". In: *International Journal of Hydrogen Energy* 32.13 (Sept. 2007), pp. 2186–2191.

[3] Florian Ettner, Klaus G. Vollmer, and Thomas Sattelmayer. "Numerical Simulation of the Deflagration-to-Detonation Transition in Inhomogeneous Mixtures". In: *Journal of Combustion* 2014 (2014), pp. 1–15.

[4] Josef Hasslberger, Lorenz R. Boeck, and Thomas Sattelmayer. "Numerical Simulation of Deflagration-to-Detonation Transition in Large Confined Volumes". In: *Journal of Loss Prevention in the Process Industries* 36 (July 2015), pp. 371–379.

[5] Mathias Henriksen et al. "A Study of The Deflagration-To-Detonation Transition and Its Limits of Hydrogen-Air Mixtures in An OpenEnded, Obstructed Channel". In: 29th ICDERS. Korea, 2023.

[6] Jeff Heylmun et al. *blastFoam Theory and User Guide Version 6*. Synthetik Applied Technologies, 2022.

[7] E. F. Toro. *Riemann Solvers and Numerical Methods for Fluid Dynamics: A Practical Introduction*. 3rd ed. Dordrecht ; New York: Springer, 2009. 724 pp.

[8] H.G. Weller et al. "Application of a Flame-Wrinkling Les Combustion Model to a Turbulent Mixing Layer". In: *Symposium (International) on Combustion* 27.1 (Jan. 1998), pp. 899–907.

[9] S. Browne et al. *SDToolbox - Numerical Tools for Shock and Detonation Wave Modeling, Explosion Dynamics Laboratory*. Explosion Dynamics Laboratory, 2021.

[10] Michéal O'Conaire et al. "A Comprehensive Modeling Study of Hydrogen Oxidation". In: *International Journal of Chemical Kinetics* 36.11 (2004), pp. 603–622.

[11] Jeff Heylmun et al. *STFS-TUDa/blastAMR: Load-balanced AMR library release (v0.1-alpha)*. 2023.

[12] M. Henriksen et al. "Numerical Study of Premixed Gas Explosion in a 1-m Channel Partly Filled with 18650 Cell-like Cylinders with Experiments". In: *Journal of Loss Prevention in the Process Industries* 77 (July 2022), p. 104761.

[13] F. R. Menter. "Two-Equation Eddy-Viscosity Turbulence Models for Engineering Applications". In: *AIAA Journal* 32.8 (Aug. 1994), pp. 1598–1605.